

Neuroprotective effect of a new free radical scavenger HL-008 against ischemia-reperfusion injury

Yahong Liu

Institute of Radiation Medicine, Chinese Academy of Medical Sciences and Peking Union Medical College

Ying Cheng

Center for Marine Bioproducts Development, College of Medicine and Public Health, Flinders University

Wei Zhang

Center for Marine Bioproducts Development, College of Medicine and Public Health, Flinders University

Hongqi Tian (✉ tianhongqi@irm-cams.ac.cn)

Institute of Radiation Medicine, Chinese Academy of Medical Sciences and Peking Union Medical College

Research Article

Keywords:

Posted Date: December 18th, 2020

DOI: <https://doi.org/10.21203/rs.3.rs-123994/v1>

License:   This work is licensed under a Creative Commons Attribution 4.0 International License.

[Read Full License](#)

Abstract

Oxidative stress plays a critical role in cerebral ischemia-reperfusion injury. We previously developed a powerful antioxidant, HL-008, and this study aimed to investigate the neuroprotective function of HL-008.

The *in vitro* and *in vivo* efficacy of HL-008 was evaluated using a PC-12 cell oxidative stress model induced by hydrogen peroxide and a rat model of middle cerebral artery occlusion, respectively. The MTT assay was used to analyze cell viability. TTC staining, HE staining, immunofluorescence, western blot, and proteomics were used to evaluate the infarction volume, brain tissue morphology, apoptosis, inflammation, and related pathways. Indicators related to oxidative levels were mainly detected using commercial kits.

HL-008 significantly reduced the cerebral infarction area induced by ischemia-reperfusion, improved the neurological score, alleviated oxidative stress and inflammation in the brain tissue, reduced glial cell activation, inhibited brain tissue apoptosis by influencing multiple signaling pathways, and had a neuroprotective effect. If HL-008 is successfully developed, it can significantly improve the quality of life of stroke patients.

Introduction

Stroke, which causes long-term disability, is the third most common cause of death after heart disease and cancer [1]. Clinically, stroke is classified as either ischemic or hemorrhagic stroke, which accounts for approximately 85% and 10% of all cases, respectively. Moreover, subarachnoid hemorrhage accounts for approximately 3% of all stroke cases [2–4]. Acute ischemic stroke (AIS), mainly caused by vascular obstruction, is treated by rapid recanalization [5, 6], which includes intravenous thrombolysis or mechanical thrombectomy. Unfortunately, the time window of intravenous thrombolytic therapy is so narrow that only 10% of patients are eligible for treatment [7]. Moreover, resumption of blood flow in the brain tissue after a certain ischemic period can cause serious secondary damage, including blood-brain barrier damage (BBB), inflammation, and neuronal damage. Following cerebral ischemia, this process is known as acute cerebral ischemia-reperfusion injury (CIRI) [4]. Therefore, there is a need for neuroprotective agents for treating AIS.

There are many types of neuroprotective agents. However, only edaravone, a reactive oxygen species (ROS) scavenger, has been confirmed as an effective treatment for AIS in Japan [8–10], which demonstrates the importance of targeting ROS in AIS treatment.

Under physiological conditions, superoxide dismutase (SOD), glutathione peroxidase, catalase (CAT), and other antioxidant enzymes can protect brain tissue through catalytic scavenging of ROS and maintain neutral balance [11]. However, during cerebral ischemia-reperfusion (I/R), mitochondrial depolarization produces numerous ROS [12, 13]. Excessive ROS can activate mitochondrial pro-apoptotic signals, induce DNA damage, and alter protein structure and function [14]. Additionally, ROS can directly regulate certain important molecules in the cellular signal pathway and damage brain tissue [15].

Although edaravone has demonstrated neuroprotective function in CIRI treatment, it is associated with fatal adverse reactions such as acute renal injury [16]. In recent years, several natural antioxidants, such as resveratrol [17], curcumin [18], ginkgo biloba [19], gallic acid [20], chalcone [21], and vitamin C and E [22, 23], have been used as dietary supplements for preventing and treating stroke. Although they are safe, they are not as effective as edaravone. Therefore, there is an urgent need to develop new and effective ROS scavengers that have neuroprotective effects on AIS.

We previously developed an ROS scavenger, HL-008. A study on radiation protection demonstrated that HL-008 had similar efficacy, but superior safety, to that of amifostine. Given the important role of ROS in CIRI, our study aimed to explore the application of HL-008 in CIRI and expand the indications for HL-008. Further, we aimed to elucidate the mechanism underlying the neuroprotective effect of HL-008 in a rat model of middle cerebral artery occlusion (MCAO).

Methods

Cell culture and treatment

Rat pheochromocytoma PC-12 cells and human embryonic kidney 293 (HEK293) cells, displaying a semi-differentiated phenotype with neuronal projections, were used as model neuronal cells. An RPMI1640 medium (Sigma-Aldrich, USA) supplemented with penicillin (100 U/mL, Sigma-Aldrich), streptomycin (100 µg/ml, Sigma-Aldrich) and 10% FBS (Scientifix Pty Ltd, French) at 37 °C in a humidified 95% air/5% CO₂ incubator was used as cell culture medium. This medium was changed daily.

Evaluation of cytotoxicity of HL-008 in vitro

Cell viability was determined by measuring the formazan produced by the reduction of MTT (No. M5665-5G, Sigma), which shows the mitochondrial activity of living cells. Cells were seeded at 1×10^4 cells per well in a 96-well plate and incubated for 24 h to allow adherence. A 1 × PBS (pH = 7.4) was first used to dissolve the HL-008 and then diluted to the final stock concentrations prior to addition to the cells. Cells were treated with the serially diluted HL-008 solution at different concentrations and then incubated for 48 h at 37 °C. Following this, the cell culture medium was replaced by 100 µL of 0.5 mg/mL MTT and incubated for 4 h. Finally, 80 µL of 20% SDS in 0.02 M HCl was added, and the plate was incubated for 18 h. The absorbance of the plate was measured at 570 nm using a microplate reader.

Evaluation of the effect of HL-008 on cytotoxicity induced by hydrogen peroxide

PC-12 cells were seeded at 1×10^4 cells per well and incubated for 24 h to allow adherence. The cells were incubated with HL-008 for 15 min prior to the addition of H₂O₂ at different concentrations (100 µM, 150 µM and 200 µM) and then incubated for 24 h at 37 °C. Following this, the medium was replaced with 0.5 mg/mL of MTT and incubated for 4 h at 37 °C. Finally, 80 µL of 20% SDS in 0.02 M HCl was added, and the plate was incubated for 18 h. The absorbance of the plate was measured at 570 nm using a microplate reader.

Animals

All male SD rats (200–300 g) used in this study were purchased from SPF Biotechnology Co., Ltd. (Beijing) and bred in a certified animal facility. The temperature in the feeding room was 24–26 °C; humidity was 37–51%; air change was performed 10–20 times/h, and the day-night alternation time was 12 h/12 h.

Ethics statement

All experimental procedures were conducted in accordance with the National Institutes of Health (NIH) Guidelines for the Care and Use of Laboratory Animals and were approved by the Institutional Animal Care and Use Committee of the Institute of Radiation Medicine, Chinese Academy of Medical Sciences (IRM, CAMS; permit number: 2017053). The animals were cared for in accordance with the guidelines of the National Animal Welfare Law of China. Meanwhile, all the studies were carried out in compliance with the Animals in Research: Reporting in vivo Experiments (ARRIVE) guidelines.

Evaluation of the BBB permeability of HL-008

The number of SD male rats used was 27. They were divided into nice groups; three rats in each group. After a single intraperitoneal injection of 200 mg/kg of HL-008, whole blood and brain were collected at 0.083, 0.25, 0.5, 1, 1.5, 2, 3, 6, and 8 h after administration. A volume of 200 µL of whole blood was collected in a blood collecting vessel containing EDTA, placed on ice, and separated at 4000 rpm for 20 min. The separated plasma was placed in a 1.5 ml EP tube. After euthanizing the rats, the brain was quickly removed. 50 µL plasma or brain tissue sample was added to 96 well plate, mixed thoroughly with 250 µL 35% trichloroacetic acid, and centrifugated at low temperature for 20 minutes. Approximately 150 µL of the supernatant was transferred to new 96-well plate and mixed with 150 µL of ultrapure water. Finally, 10 µL of the sample was obtained to enter into the LC-MSMS system (API4000 Q-Trap).

Establishment of an animal model of AIS

The AIS model was established by MCAO in the rats. The body temperature of the anesthetized rats was maintained at 37 ± 0.5 °C. With a median cervical incision, the distal end of the external carotid artery was ligated with a 6 – 0 silk thread, 4 mm from the common carotid artery bifurcation. Another 6 – 0 silk thread was inserted into the external carotid artery, and a living knot was made near the common carotid artery bifurcation. A head-treated 0.33 mm diameter nylon wire was then inserted into the middle cerebral artery. The insertion depth of the nylon wire was approximately 16 ± 1 mm at the bifurcation of the common carotid artery. After ischemia, at 90 min, the thread bolt was removed, the proximal end of the external artery with 6 – 0 silk thread was ligated, and the neck wound was sutured with 3 – 0 silk thread. The rats were then placed on a heating pad.

Evaluation the protective effect of HL-008 on the MCAO model

A total of 25 male SD rats (200–250 g) were divided into five groups (n = 5 each), including a control group, ischemia reperfusion (I/R) group, HL-008 100 mg/kg group, HL-008 50 mg/kg group, and HL-008 25 mg/kg group. During reperfusion, HL-008 was administered intravenously. After 24 h of reperfusion, the neurological function score and cerebral infarction area were evaluated.

Assessment of neurological deficits and the infarct area

The neurological behaviors were evaluated based on Longa and Bederson's 5-point scoring system [24–26]; 0, observed behavioral deficits; 1, unable to fully extend the opposite forepaw; 2, failure to turn to the opposite side; 3, falling to the opposite side; 4, no spontaneous walking. The higher the score, the more serious the neurological impairment of the animal.

For assessment of infarct volume, the brain tissue of rats was obtained and cut into 2 mm thick slices along the coronal plane after neurological scoring. Half of the brain slices were placed into 2% TTC dye solution at intervals. After incubation at 37 °C for 10 min, the slices were turned regularly for uniform staining. The normal brain tissue was bright red and the infarcted area was pale in color. The infarct area was measured and analyzed by Image Pro Plus 6.0 software.

Comparison of efficacy between HL-008 and edaravone

A total of 20 male SD rats (200–250 g) were divided into four groups (n = 5 each), including a control group, ischemia reperfusion (I/R) group, HL-008 100 mg/kg group and edaravone 3 mg/kg group. During reperfusion, HL-008 and edaravone were administered intravenously. After 24 h of reperfusion, the neurological function score and cerebral infarction area were evaluated.

Investigation of the HL-008 mechanism

A total of 15 male SD rats (200–250 g) were divided into three groups (n = 5 each), including a control group, ischemia reperfusion (I/R) group, and HL-008 100 mg/kg group. During reperfusion, HL-008 and edaravone were administered intravenously. After 24 of reperfusion, the rats were killed and the brain tissue was removed for further study.

Measurement of ROS levels in the brain

Brain tissue weighing 0.1 g was fully homogenized with 1 mL of extracting solution on ice and centrifuged at 10000 g and 4 °C. The supernatant was obtained and placed on ice for testing. The ROS content in the brain tissue was analyzed using an ROS detection kit (No. E004, Nanjing Jiancheng Bioengineering Institute, China). The procedure was conducted according to manufacturer's instructions.

Evaluation of malondialdehyde (MDA) in the brain

Brain tissue weighing 0.1 g was fully homogenized with 1 mL of extracting solution on ice and centrifuged at 8000 g, at 4 °C, for 20 min. The supernatant was obtained and placed on ice for testing. The MDA content in brain tissue was analyzed using an MDA detection kit (No. X-W-A401, Sino Best Biological Technology Co., Ltd., China), according to the manufacturer's instructions.

Evaluation of antioxidant activity

Brain tissue weighing 0.1 g was fully homogenized with 1 mL of extracting solution on ice and centrifuged at 10000 g, at 4 °C for 20 min. The supernatant was obtained and placed on ice for testing. The activities of SOD (No. YX-W-A500, Sino Best Biological Technology Co., Ltd., China), CAT (YX-W-A501, Sino Best Biological Technology Co., Ltd., China), and GSH-Px (A005, Nanjing Jiancheng Bioengineering

Institute, China) in rat brain tissues were tested using commercial kits, according to the manufacturer's instructions.

Hematoxylin and eosin (HE) staining

The brain tissue samples fixed with 4% paraformaldehyde, were embedded in paraffin, and cut into 5 μm sections using a paraffin slicer. After slicing, the slices were slightly dried in air and baked overnight in an oven at 60 $^{\circ}\text{C}$. After the slices were successfully obtained, they were dewaxed with xylene and absolute ethanol to water, then stained with HE (71014460; Shanghai Jingke Chemical Technology Co., Ltd.) and analyzed using the Panoramic SCAN (3D HISTECH). The nucleus was dyed blue and the cytoplasm dyed red. Based on the staining results in each group, the morphological changes were analyzed.

Analysis of TUNEL staining

The paraffin section was dewaxed with xylene and absolute ethanol to water. A concentration of 20 $\mu\text{g}/\text{ml}$ protease K without DNase was added at 20–37 $^{\circ}\text{C}$ for 15–30 min. After washing thrice with PBST, each slice was added to 50 μL of TUNEL reaction solution (No. 11684795910, Roche) and incubated in a constant temperature incubator at 37 $^{\circ}\text{C}$ in the dark for 60 min. Each slice was washed thrice with PBST and combined with 100 μL 4',6-Diamidino-2-phenylindole (DAPI, 1:1000 PBS pH = 7.4), away from light for 10 min at room temperature. Finally, PBST (pH = 7.4) was used to wash the slices thrice, and a fluorescence quenching agent was used to seal the slices for microscopic inspection (Panoramic SCAN, 3D HISTECH). DAPI was stained with blue fluorescence in the nucleus and green fluorescence in the positive part.

Immunofluorometric assay

The fixed tissue sections were dewaxed to water; washed with PBS thrice for 3 min each; blocked by 0.3% hydrogen peroxide; incubated at room temperature for 20 min; washed by PBS again thrice for 3 min each, using 0.01 M citric acid (pH 6.0) buffer solution for antigen repair. After natural cooling, they were washed with PBS (pH = 7.4) thrice, for 3 min each, and dripped and sealed with normal goat serum at 37 $^{\circ}\text{C}$ for 30 min. The serum was poured out, and 1:100 diluted TNF- α (No. Ab167161, abcam), IL-1 β (No. Ab8348, abcam) and 1:300 diluted GFAP (No. Ab68428, abcam) antibody were added and incubated overnight at 4 $^{\circ}\text{C}$. They were then washed thrice with PBS, and a 1:200 diluted fluorescent coupling antibody was added and incubated for 1 h in the dark at room temperature. The nucleus was then dyed with DAPI, washed thrice with PBS, sealed with 50% buffer glycerin, and observed using fluorescence microscopy during which photographs were obtained.

Western blotting

The tissue was washed with cold PBS (pH = 7.4) twice or thrice, cut into small pieces, and homogenated. Add 10 times the tissue volume of lytic fluid (add protease inhibitor a few minutes before use) to the ice for complete homogenization. The supernatant was collected by centrifugation of 12000 g for 5 min, resulting in the total protein solution. The protein concentration was measured using the BCA method, and the protein was separated using SDS-PAGE electrophoresis. After electrophoresis, the blocked membrane was incubated using the first antibody, including Nrf2 (No. AF0639, Affinity), HO-1 (No.

AF5393, Affinity), Bax (No. AF0120, Affinity), Caspase-3 (No. AF6311, Affinity), P-p38(No. AF4001, Affinity), p-NF- κ B (No. AF2006, Affinity), Bcl-2(No. AF6193, Affinity), p-ERK (AF1015, Affinity), p-JNK (AF3318, Affinity), P-p53(AF3075, Affinity), NOX4 (DF6924, Affinity), and GAPDH (ab 68428, Abcom). Following this, the second antibody was incubated. The chemiluminescent substrate was dripped onto the membrane and incubated in a dark room for approximately 5 min. The luminous substrate was discarded, the film was placed between X-ray films of equal size, and exposed for approximately 1–3 min. Then an X-ray film was taken out every other minute. Finally, the X-ray film was developed for 5 minutes, fixed for 5 minutes, and washed for more than 10 min and dried.

Proteomic analysis

The tissue samples were ground into powder with liquid nitrogen, and 6 mL of protein extract I (40 g trichloroacetic acid + 400 mL protein extract II, -20 °C, 1 h) was added, and centrifuged at 4 °C, 12000 rpm for 20 min. Following this, 6 mL of protein extract II (400 mL acetone + 280 μ L β -mercaptoethanol, -20 °C, 1 h) was added to the precipitate, and centrifuged at 4 °C 12000 rpm for 20 min. The precipitate was vacuumed dry to obtain the crude protein powder. Then, a certain amount of dry powder was added to 400 μ L of the SDT (8 M urea, 100 mM Tris-HCl, 1 mM PMSF, PH = 8.5) cracking solution for dissolution, and placed at room temperature for 1 h. Centrifugation at 9000 rpm at 4 °C for 10 min was performed to obtain the protein sample. The protein concentration was determined using the Bradford method and identified by SDS-PAGE. The total protein was hydrolyzed with trypsin in an incubator set at 37 °C for 12–16 h. The hydrolysate was washed with 50 mM of ammonium bicarbonate, acidified with trifluoroacetic acid (TFA), vibrated, centrifuged to remove sodium deoxycholate (SDC), and desalinated with the C18 column. The desalted samples were lyophilized in a freeze-drying apparatus, then re-dissolved in 0.1% formic acid after lyophilization, and detected using a mass spectrometer (Q-active mass spectrometer, Thermo Fisher). The retrieved proteomic database was from the UniProt, *Rattus norvegicus* (rat) protein, with a 29944 protein count. Maxquant (version 1.6.0.1) and Protein Discoverer (edition 1.4) were used for database retrieval and relative quantification.

Results

HL-008 shows no cytotoxicity on PC-12 cells and HEK293 cells

The cytotoxicity of HL-008 was measured using the MTT assay in PC-12 and HEK293 cells. HL-008, over a range of concentrations, did not show any statistically significant cytotoxicity over 48 h, and the cell viability was typically > 90% (Fig. 1A and B).

Neuroprotective effect of HL-008 against H₂O₂-induced cytotoxicity in vitro

The neuroprotective activity of HL-008 *in vitro* was evaluated using PC-12 cells. At all tested concentrations of H₂O₂ pretreatment, cells with HL-008 showed a dramatically increased viability in a concentration-dependent manner up to 100%. H₂O₂ at 100 μ M induced cytotoxicity of approximately 53% when the cells were treated for 24 h. Pretreating the cells with HL-008 at concentrations from 100 μ M to

400 μM however dramatically reduced the cytotoxicity ($p < 0.01$ or $p < 0.001$). Likewise, H_2O_2 at 150 μM induced cytotoxicity of approximately 62%, while pretreating the cells with HL-008 at concentrations of 150 μM to 400 μM significantly increased viability ($p < 0.001$). Similarly, H_2O_2 at 200 μM induced cytotoxicity of approximately 64%, while pretreating the cells with HL-008 at concentrations from 200 μM to 400 μM reduced the cytotoxicity to 22% and 0.5%, respectively, suggesting significant neuroprotective effects ($p < 0.001$). This result is shown in Fig. 1C, D, and E.

HL-008 can enter the brain tissue through BBB

In vitro, HL-008 can penetrate the cell membrane and play a protective role in nerve cells. However, the BBB is a special structure in brain tissue. Many neuroprotective agents show good efficacy *in vitro*, but studies on these agents had to be terminated because they could not penetrate the BBB. Therefore, we evaluated the permeability of HL-008, and the results are shown in Fig. 2 and Table S1. The BBB permeability of HL-008 is 35%, indicating that HL-008 can penetrate the BBB and enter the brain tissue.

HL-008 alleviated reperfusion injury in MCAO model rats

In order to evaluate whether HL-008 has a protective effect on ischemia-reperfusion injury *in vivo*, MCAO rats were treated with different concentrations of HL-008. The results are shown in Fig. 3. Among the HL-008 groups, the neurological scale was lower in the I/R group ($p < 0.01$, Fig. 3A). Behavioral improvement was 60.00%, 66.67%, and 66.67% in the HL-008 100, 50, and 25 mg/kg groups, respectively (Table S2). The infarction volume was evaluated with TTC staining and was significantly lesser in the HL-008 groups than in the I/R groups 24 h after reperfusion ($p < 0.00$, Fig. 3B and C). Improvement in cerebral infarction volume was 86.88%, 83.75% and 84.13% in the HL-008 100, 50, and 25 mg/kg groups, respectively (Table S2).

HL-008 has a stronger neuroprotective effect than edaravone

The neuroprotective effects of HL-008 were compared with the positive control edaravone. The results showed that HL-008 and edaravone significantly improved the neurological function score and infarct size in MCAO rats. There were significant differences between the two groups compared with the I/R group (neurological score: HL-008 vs I/R, $p < 0.001$; edaravone vs I/R, $p < 0.05$; infarction volume: HL-008 vs I/R, $p < 0.0001$; edaravone vs I/R, $p < 0.001$; Fig. 4). Most importantly, the neuroprotective effect of HL-008 was stronger than that of edaravone, and there were significant differences (neurological score: HL-008 vs edaravone, $p < 0.01$; infarction volume: HL-008 vs edaravone, $p < 0.05$; Fig. 4). The specific values are shown in Table S3.

HL-008 relieves oxidative stress in the brain tissues of MCAO rats

We evaluated the level of oxidation in the brain of MCAO rats, including the level of ROS and MDA. The results showed that HL-008 could significantly reduce the level of ROS in the brain of MCAO rats ($p < 0.05$, Fig. 5A) and alleviate the level of MDA - a marker of lipid peroxidation. The difference was significant ($p < 0.05$, Fig. 5B). Meanwhile, the results of a study on the antioxidant enzyme system in the brain tissue of

MCAO model rats showed that HL-008 can increase the levels of antioxidant enzymes SOD (HL-008 248.50 ± 7.30 vs I/R 160.09 ± 9.88 U/g), CAT (HL-008 745.84 ± 58.02 vs I/R 400.17 ± 24.83 U/g), and GSH-Px (HL-008 3.14 ± 0.37 vs I/R 1.87 ± 0.19 U/g, and the differences were statistically significant ($p < 0.001$, $p < 0.001$, $p < 0.01$, respectively. Figure 5C, D, and E).

HL-008 alleviates the histopathological changes induced by reperfusion

The histopathological changes in each group were observed on HE staining, and the results are shown in Fig. 6A. In the control group, the brain tissue structure and the morphology of nerve cells were normal. The nerve cells had a clear outline, the nucleus was round, and the nucleolus clearly visible. However, in the cerebral tissue in the I/R group, there were vacuoles of various sizes, and a shrunken and deformed nucleus was observed. Compared with the I/R group, the structure of the neurons in the HL-008 group was more regular, the nucleus was visible, the vacuolation was smaller, and no obvious damage was observed.

HL-008 ameliorates cell apoptosis in brain tissues

TUNEL staining was performed to assess cell apoptosis in rat brain tissue, 24 h after ischemia reperfusion. The results are shown in Fig. 6B. The TUNEL-positive green cells represented the apoptosis cells. The number of apoptotic cells was significantly increased in the I/R group, compared with the control group. These changes were attenuated by HL-008 treatment, as evidenced by the decreased number of TUNEL-positive cells.

HL-008 reduces the GFAP level in brain tissues

We evaluated the effect of HL-008 on the GFAP level in brain tissue 24 h after reperfusion, and the result is shown in Fig. 7. Compared with the control group, the number of GFAP positive cells in the brain tissue showed an upward trend in the I/R group. HL-008 can reduce the level of GFAP after cerebral ischemia-reperfusion. We also observed the effect of HL-008 on the changes in pro-inflammatory cytokines in brain tissue 24 h after reperfusion. Unfortunately, compared with the control group, we did not observe any changes in the levels of TNF and IL-1 β in the brain tissue of MCAO rats, including the I/R group. The specific reason is not yet clear (data not shown).

HL-008 exerts neuroprotective function by regulating multiple pathways

In order to evaluate the neuroprotective effect of HL-008 24 h after reperfusion, and according to the results described above, the expression level of the related pathway proteins was detected using the western blot assay. The results are shown in Fig. 8A and Figure S1. I/R injury increased the expression of proteins Bax, Caspase-3, P-p53, p-JNK, p-38, NF- κ B, and NOX4, and decreased the expression of proteins Bcl-2, Nrf-2, HO-1, and p-ERK. It is noteworthy that the expression levels of proteins increased by I/R injury were downregulated after HL-008 treatment, and the expression levels of proteins decreased by I/R injury were upregulated after HL-008 treatment.

Proteomic analysis

We used proteomics to explore other possible pathways involved in the neuroprotective function of HL-008 and the regulatory-related proteins; 2167 proteins were identified with different expressions. In the I/R

versus control, HL-008 vs control, and HL-008 vs I/R, there were 214, 273, 161 upregulated proteins, and 197, 354, 383 downregulated proteins (fold change ≥ 1.2 , Figure S2). For each identified protein, we performed GO enrichment analysis. The results are presented in a heat map (Figure S3). Bioinformatic analysis of three levels, biological process, cellular component, and molecular function, showed that top 10 biological processes in I/R versus control, HL-008 vs control, and HL-008 vs I/R, respectively (Figure S4). In particular, the pathway for glycerophospholipid metabolism attracted our attention (Figure S5). Based on the analysis of ≥ 1.2 -fold upregulated and downregulated proteins, we identified two proteins that may be associated with the neuroprotective function of HL-008, including relational-binding protein (RBP4), and serum albumin (Fig. 8B and C). RBP4 is the specific carrier for retinol (vitamin A) in the blood and associated with a short-term prognosis in ischemic stroke, and serum albumin is associated with inflammation in ischemia-reperfusion injury. HL-008 can significantly inhibit the increase of RBP4 and serum albumin expression induced by ischemia-reperfusion.

Discussion

Since 1996, tissue plasminogen activator (tPA) has been the only FDA-approved medication for mainstay treatment of AIS. The tissue plasminogen activator, tPA dissolves thrombi and restores blood flow by promoting fibrinolysis. However, there is increasing evidence indicating that an ROS burst caused by reperfusion may aggravate brain injury [27–29]. Therefore, timely and effective ROS elimination in the I/R process is favorable for neuroprotection.

HL-008 exhibited significant neuroprotective effects *in vivo* and *in vitro*, effectively reversed the I/R-induced redox imbalance, and alleviated brain morphological changes, including shrinkage, vacuolation, and blood vessel congestion. During ischemia-reperfusion, an ROS burst often induces neuroinflammation, including activation of astrocytes and microglia [30]. Astrocytes are associated with multiple functions in the central nervous system [31]. In response to physiological changes, particularly acute and sub-acute tissue responses to injury, astrocytes are activated and function as key players [32–33]. Reactive astrocyte activation induces changes in gene expression, including GFAP upregulation. Increased GFAP expression is an important marker of astrocyte activation [34]. Moreover, inflammation is related to upregulation of astrocytosis [35]. HL-008 significantly alleviated astrocyte activation, reversed the increase in serum albumin levels in brain tissue, and deregulated the increased NF- κ B expression, suggesting that HL-008 treatment has anti-inflammatory effects.

NOX4, as a member of the NOx family, induces brain injury by converting O₂ into ROS and plays a highly specific role in I/R. NOX4 inhibition has a critical role in maintaining BBB stability [36]. HL-008 not only effectively eliminates ROS, but also reduces ROS production by inhibiting of NOX4 expression, thus reducing ROS-induced brain tissue damage.

Apoptosis is among the important mechanisms of neuronal death in AIS [37]. ROS produced during I/R can induce DNA damage; activate p53; interfere with an interaction between Bcl-2 and Bax; open mitochondrial pores; release apoptosis-promoting factors, including cytochrome c; activate caspase 3/9

cascade reaction; and finally induce apoptosis [38]. HL-008 reversed the increase in P-p53, Bax, and caspase-3 protein expression, and reduced I/R-induced Bcl-2 protein expression. Further, TUNEL staining confirmed that HL-008 inhibited I/R-induced apoptosis.

The Nrf2/HO-1 pathway is critically involved in oxidative stress. Under oxidative stress, Nrf-2 is dissociated from Keap1; enters the nucleus; and promotes the expression of antioxidant proteins, including SOD and HO-1 [39]. HL-008 significantly promoted Nrf2 and HO-1 protein expression. Moreover, Nrf-2 can be activated by MAPK kinase pathways. ERK1/2, p38 MAPK, and JNK signaling over-activation has been reported in AIS. Moreover, ERK1/2, p38, and JNK phosphorylation inhibition can relieve brain injury. HL-008 can significantly alleviate the excessive activation of ERK1/2, p38, and JNK after ischemia-reperfusion, as well as reduce the severity of brain injury.

Proteomic analysis suggested a close association of RBP4 proteins with the neuroprotective effect of HL-008. Increased RBP4 levels are associated with AIS severity and prognosis of AIS [40]. I/R induced a significant expression of RBP4 protein, which was inhibited by and HL-008. These findings could provide new ideas for future research.

There are also some limitations in this study. First of all, there is no completely simulate the situation of real clinical patients in the currently used rat model of cerebral stroke ischemia-reperfusion injury. At the same time, due to species differences, the results of this study can not be directly translated to clinical patients. Therefore, we need to explore new animal models to meet the clinical needs. Secondly, although we have done the study of protein spectrum, but we have not verified the related altered proteins, but this will be the focus of our next work. Finally, we only evaluated NOX4, a protein that affects the stability of BBB, and did not discuss other stability indicators with BBB, such as the change of BBB permeability, which we will study in depth in the future.

Declarations

Acknowledgments

This work was supported by the Tianjin Major Scientific and Technological Projects of New Drug Creation [17ZXXYSY00090], Technological Support Projects of the Tianjin Key R&D Program [19YFZCSY00350], and Cotutelle PhD scholarship from Flinders University, with research support from the Centre for Marine Bioproducts Development, Flinders University.

Author contributions statement

Hongqi Tian and Wei Zhang conceived and designed the experiments; Yahong Liu and Ying Cheng performed the experiments; Yahong Liu analyzed and interpreted the results and prepared the manuscript; and Ying Cheng contributed to the manuscript preparation and data analysis. All authors have revised and read the manuscript.

Conflicts of Interest

The authors declare that they have no conflicts of interest.

References

1. Kim, Y., Park, J., Lee, J. E., Yenari, M. A. NOX Inhibitors-A promising avenue for ischemic stroke. *Exp. Neurobiol.* **26**, 195-205 (2017) .
2. World Health Organization, Top ten causes of death, <http://www.who.int/mediacentre/factsheets/fs310/en/index.html>. (accessed August 19, 2012)
3. Zhang, Y., Wang, Z. J., Miao, L., Wang, Y., Chang, L. L., Guo, W., Zhu, Y. Z. Neuroprotective effect of SCM-198 through stabilizing endothelial cell function. *Oxid. Med. Cell Longev.* 7850154 (2019).
4. Radermacher, A., Wingler, K., Langhauser, F., Altenhöfer, S., Kleikers, P., Hermans, J. J. R., Angelis, de M. H., Kleinschnitz, C., Schmidt, H. H. W. Neuroprotection after stroke by targeting NOX4 as a source of oxidative stress. *Antioxid. Redox Signal.* **18**, 1418-1427 (2013) .
5. Zhang, Q. , Wang, Z. J., Sun, D. M., Wang, Y., Xu, P., Wu, W. J., Liu, X. H., Zhu, Y. Z. Novel therapeutic effects of leonurine on ischemic stroke: new mechanisms of BBB integrity. *Oxid. Med. Cell Longev.* 7150376 (2017).
6. Jahan, Hyperacute therapy of ischemic stroke: intravenous thrombolysis. *Tech. Vasc. Interv. Radiol.* **8**, 81-86 (2005).
7. Liu, , Wang, Y., Akamatsu, Y., Lee, C. C., Stetler, R. A., Lawton, M. T., Yang, G. Y. Vascular remodeling after ischemic stroke: mechanisms and therapeutic potentials. *Prog Neurobiol.* **115**, 138-156 (2014).
8. Shinohara, , Inoue, S. Cost-effectiveness analysis of the neuroprotective agent edaravone for noncardioembolic cerebral infarction. *J. Stroke Cerebrovasc. Dis.* **22**, 668-674 (2013).
9. Tsukamoto, , Takizawa, S., Takahashi, W., Mase, H., Miyachi, H., Miyata, T., Takagi, S. Effect of edaravone on the estimated glomerular filtration rate in patients with acute ischemic stroke and chronic kidney disease. *J. Stroke Cerebrovasc. Dis.* **20**, 111-116 (2011).
10. Watanabe, , Taham, M., Todo, S. The novel antioxidant edaravone: from bench to bedside. *Cardiovasc Ther.* **26**, 101-114 (2008).
11. J. Robinson, D.R. Winge, Copper metallochaperones, *Annual Review of Biochemistry*, 79 (2010) 537-562.
12. Shenoda, The role of Na⁺/Ca²⁺ exchanger subtypes in neuronal ischemic injury. *Transl Stroke Res.* **6**, 181-190 (2015).
13. Walder, E., Green, S. P., Darbonne, W. C., Mathias, J., Rae, J., Dinauer, M. C., Curnutte, J. T., Thomas, G. R. Ischemic stroke injury is reduced in mice lacking a functional NADPH oxidase. *Strok.* **28**, 2252-2258 (1997).
14. Granzotto , Sensi, S. L. Intracellular zinc is a critical intermediate in the excitotoxic cascade. *Neurobiol. Dis.* **81**, 25-37 (2015).
15. Wang, , Reece, E. A., Yang, P. Advances in revealing the molecular targets downstream of oxidative stress-induced proapoptotic kinase signaling in diabetic embryopathy. *Am. J. Obstet. Gynecol.* **213**,

- 125-134 (2015).
16. Feng, , Yang, Q., Liu, M., Li, W. Z., Yuan, W., Zhang, S.H., Wu, B., Li, J. Edaravone for acute ischaemic stroke. *Cochrane Systematic Review*. CD007230 (2011).
 17. Ren, , Fan, C., Chen, N., Huang, J., Yang, Q. Resveratrol pretreatment attenuates cerebral ischemic injury by upregulating expression of transcription factor Nrf2 and HO-1 in rats. *Neurochem. Res.* **36**, 2352-2362 (2011).
 18. Liu, , Ran, Y., Huang S., Wen, S. H., Zhang, W. X., Liu, X. R., Ji, Z. L., Geng, X. K., Ji, X. M., Du, H. S., Leak, R. K., Hu, X. M. Curcumin protects against ischemic stroke by titrating microglia/macrophage polarization. *Front Aging Neurosci.* **9**, 233 (2017).
 19. Li, , Zhang, X., Fang, Q., Zhou, J. S., Zhang, M. J., Wang, H., Chen, Y., Xu, B.Y., Wu, Y.F., Qian, L., Xu, Y. Ginkgo biloba extract improved cognitive and neurological functions of acute ischaemic stroke: a randomised controlled trial. *Stroke Vasc. Neurol.* **2**, 189-197 (2017).
 20. Zhao, , Li, D., Zhu, Z., Sun, Y. Improved neuroprotective effects of gallic acid-loaded chitosan nanoparticles against ischemic stroke. *Rejuvenation Res.* (2019).
 21. Wang, , Huang, L., Cheng, C., Li, G., Xie, J. W., Shen, M. G., Chen, Q., Li, W.L., He, W. F., Qiu, P. H., Wu, J. Z. Design, synthesis and biological evaluation of chalcone analogues with novel dual antioxidant mechanisms as potential anti-ischemic stroke agents. *Acta Pharm. Sin B.* **9**, 335-350 (2019).
 22. Ullegaddi, , Powers, H. J., Gariballa, S. E. Antioxidant supplementation enhances antioxidant capacity and mitigates oxidative damage following acute ischaemic stroke. *Eur. J. Clin. Nutr.* **59**, 1367-1373 (2005).
 23. Mishima, , Tanaka, T., Pu, F., Egashira, N., Iwasaki, K., Hidaka, R., Matsunaga, K., Takata, J., Karube, Y., Fujiwara, M. Vitamin E isoforms alpha-tocotrienol and gamma-tocopherol prevent cerebral infarction in mice. *Neurosci. Lett.* **337**, 56-60 (2003).
 24. Longa, Z., Weinstein, P. R., Carlson, S., Cummins, R. Reversible middle cerebral artery occlusion without craniectomy in rats. *Stroke.* **20**, 84-91 (1989).
 25. Yenari, A., Xu, L., Tang, X. N., Qiao, Y., Giffard, R. G. Microglia potentiate damage to blood-brain barrier constituents: improvement by minocycline in vivo and in vitro. *Stroke.* **37**, 1087-1093 (2006).
 26. Wang, , Zhang, Y., Wu, L., Wang, Y.J., Cao, Y. J., He, L. C., Li, X., Zhao, J. J. Puerarin protected the brain from cerebral ischemia injury via astrocyte apoptosis inhibition. *Neuropharmacology.* **79**, 282-289 (2014).
 27. Pua, J., Shi, Y. J., Zhang, L. L., Lu, Z. Y., Ye, Q., Leak, R. K., Xu, F., Ma, S. B., Mu, H. F., Wei, Z. S., Xu, N., Xia, Y. G., Hu, X. M., Hitchens, T. K., Bennett, M. V. L., Chen, J. Protease-independent action of tissue plasminogen activator in brain plasticity and neurological recovery after ischemic stroke. *Proc. Natl. Acad. Sci. U. S. A.* **116**, 9115-9124 (2019).
 28. Waldma, , Tadi, P., Rawal, A. R. Stroke Center Certification. *StatPearls.* (2019).
 29. Wang, , Mao, J. Q., Wang, R., Li, S. N., Wu, B., Yuan, Y. F. Kaempferol protects against cerebral ischemia reperfusion injury through intervening oxidative and inflammatory stress induced apoptosis. *Front Pharmacol.* **11**, 424 (2020).

30. González, F., Baltuch, G. Microglia as mediators of inflammatory and degenerative diseases. *Annu. Rev. Neurosci.* **22**, 219-240 (1999).
31. Peknya, , Pekna, M. Reactive gliosis in the pathogenesis of CNS diseases. *Biochimica et Biophysica Acta* **1862**, 483-491 (2016).
32. Sofroniew, V. Molecular dissection of reactive astrogliosis and glial scar formation. *Trends Neurosci.* **32**, 638-647 (2009).
33. Buffo, , Rolando, C., Ceruti, S. Astrocytes in the damaged brain: molecular and cellular insights into their reactive response and healing potential. *Biochem. Pharmacol.* **79**, 77-89 (2010).
34. Pekny, , Wilhelmsson, U., Tatlisumak, T., Pekna, M. Astrocyte activation and reactive gliosis-a new target in stroke? *Neurosci. Lett.* **689**, 45-55 (2019).
35. Wang, , Yao, M. J., Liu, J. X., et al. Ligusticum chuanxiong exerts neuroprotection by promoting adult neurogenesis and inhibiting inflammation in the hippocampus of ME cerebral ischemia rats. *J. Ethnopharmacol.* **249**, 112385 (2020).
36. Casas, I., Geuss, E., Kleikers, P. W. M., et al. NOX4-dependent neuronal autotoxicity and BBB breakdown explain the superior sensitivity of the brain to ischemic damage. *Proc. Natl. Acad. Sci. U. S. A.* **114**, 12315-12320 (2017) .
37. Radak, , Katsiki, N., Resanovic, I., et al. Apoptosis and acute brain ischemia in ischemic stroke. *Curr. Vasc. Pharmacol.* **15**, 115-122 (2017).
38. Srinivasa, S., Tana, B. W. Q., Vellayappanb, B. A., Jeyasekharana, A. D. ROS and the DNA damage response in cancer. *Redox. Biol.* **25**, 101084 (2019).
39. Shin, J., Chung, Y. H., Le, H. L. T., et al. Melatonin attenuates memory impairment induced by klotho gene deficiency via interactive signaling between MT2 receptor, ERK, and Nrf2-related antioxidant potential. *Int. J. Neuropsychopharmacol.* **18**, 105 (2014).
40. Zhu, Y., Zhang, J. L., Liu, L., et al. Evaluation of serum retinol-binding protein-4 levels as a biomarker of poor short-term prognosis in ischemic stroke. *Biosci. Rep.* **38**, BSR20180786 (2018).

Figures

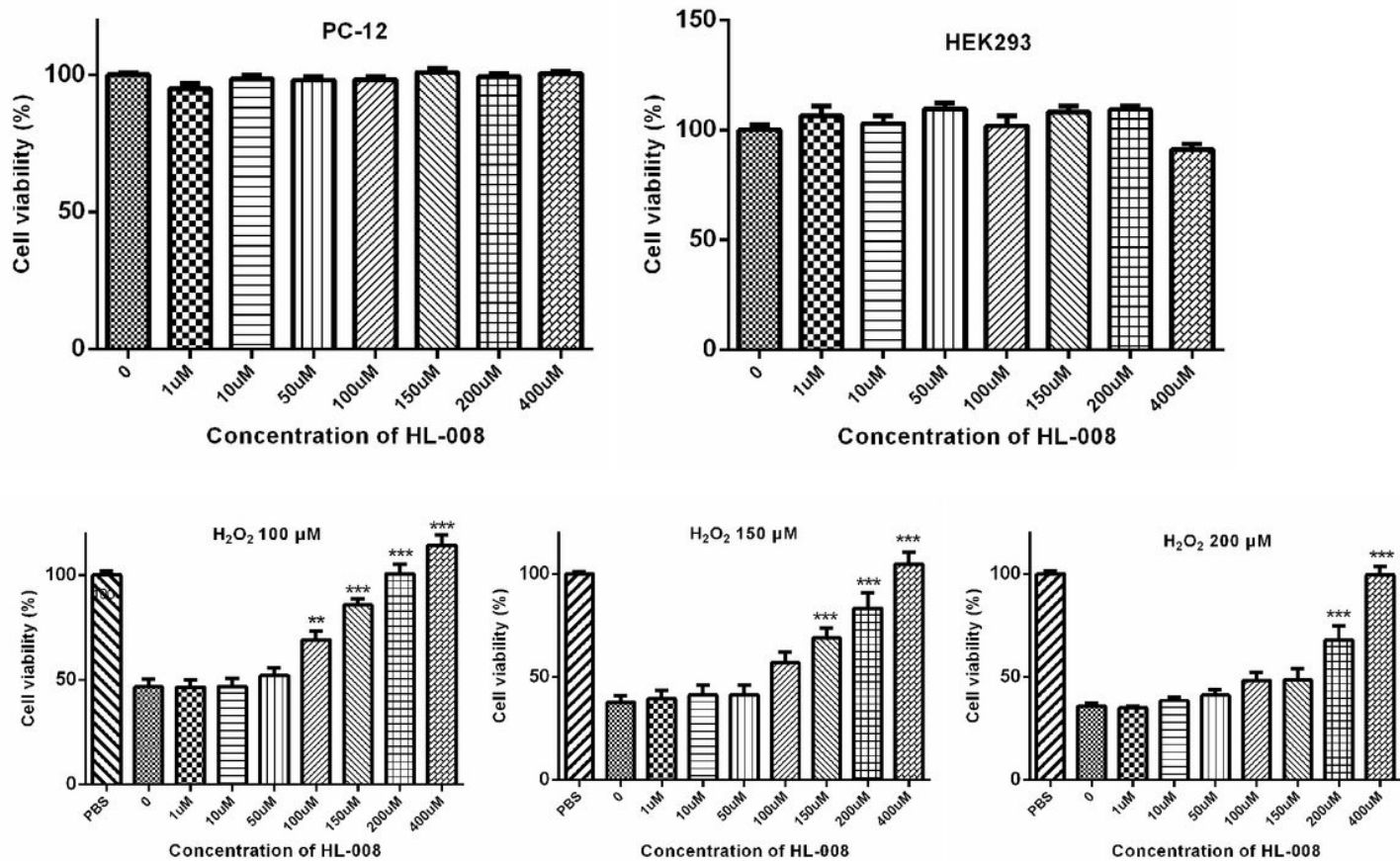


Figure 1

Relative cell viability (%) of PC-12 cells and HEK293 cells determined by MTT assay following an 48 h treatment with different concentrations of HL-008; Evaluation of the protective effects of HL-008 on PC-12 cells at different concentrations of H₂O₂: C 100 μM; D 150 μM; E 200 μM. *p < 0.05, **p < 0.01, ***p < 0.001.

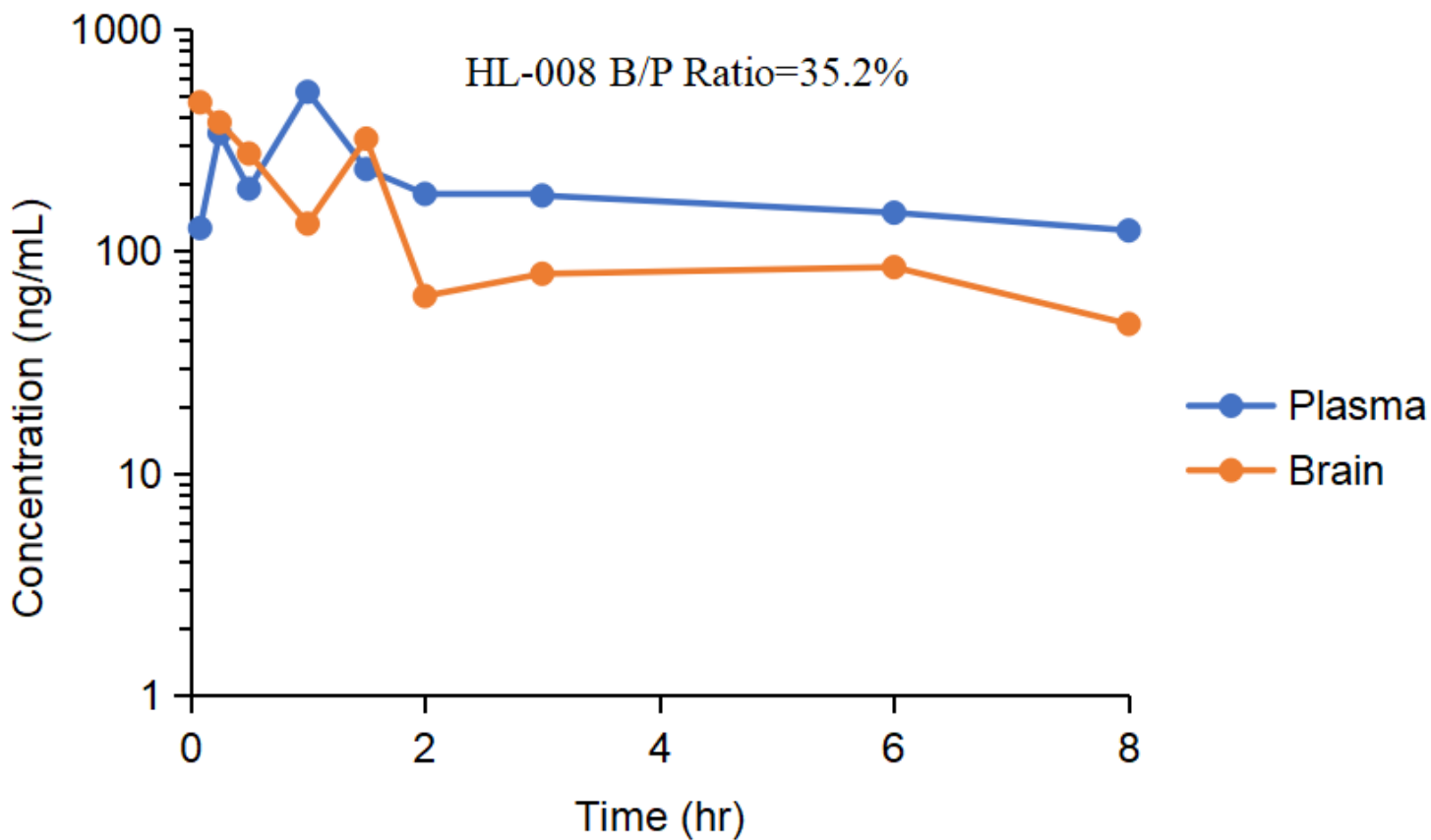


Figure 2

HL-008 permeability of BBB. SD male rats were treated with 200 mg/kg HL-008 by intraperitoneal injection, and the samples were collected at 0.083, 0.25, 0.5, 1, 1.5, 2, 3, 6, and 8 h after administration and analyzed using an LC-MSMS system.

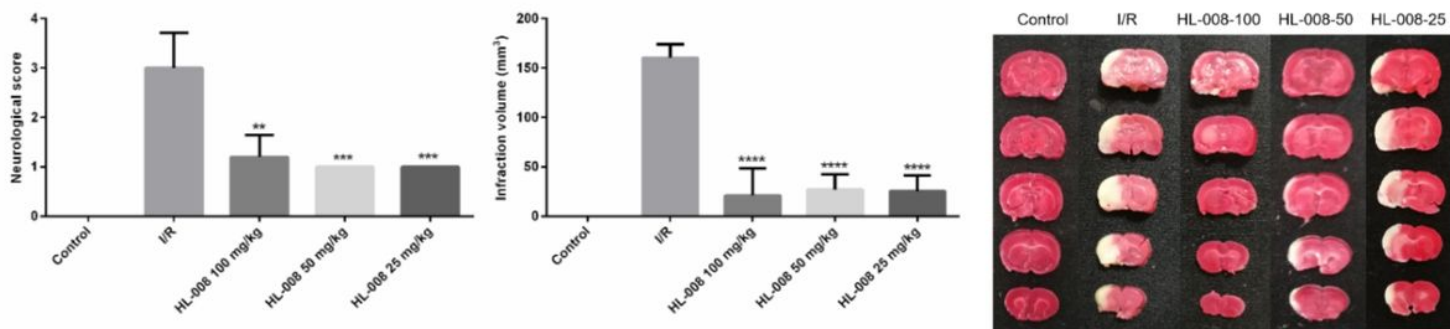


Figure 3

Pharmacodynamic evaluation of different doses of HL-008 on reperfusion injury in MCAO rats : A, Neural function score histogram; B, Cerebral infarction volume histogram; C, TTC staining. * $p < 0.05$, ** $p < 0.01$, *** $p < 0.001$.

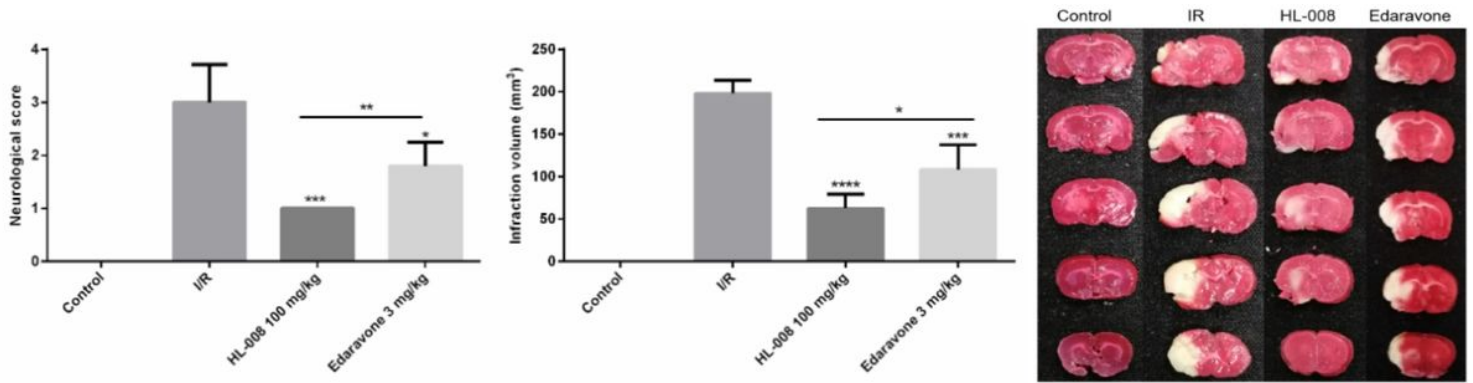


Figure 4

Comparison of the efficacy between HL-008 and edaravone on MCAO rats. A, Neural function score histogram; B, Cerebral infarction volume histogram; C, TTC staining. * $p < 0.05$, ** $p < 0.01$, *** $p < 0.001$.

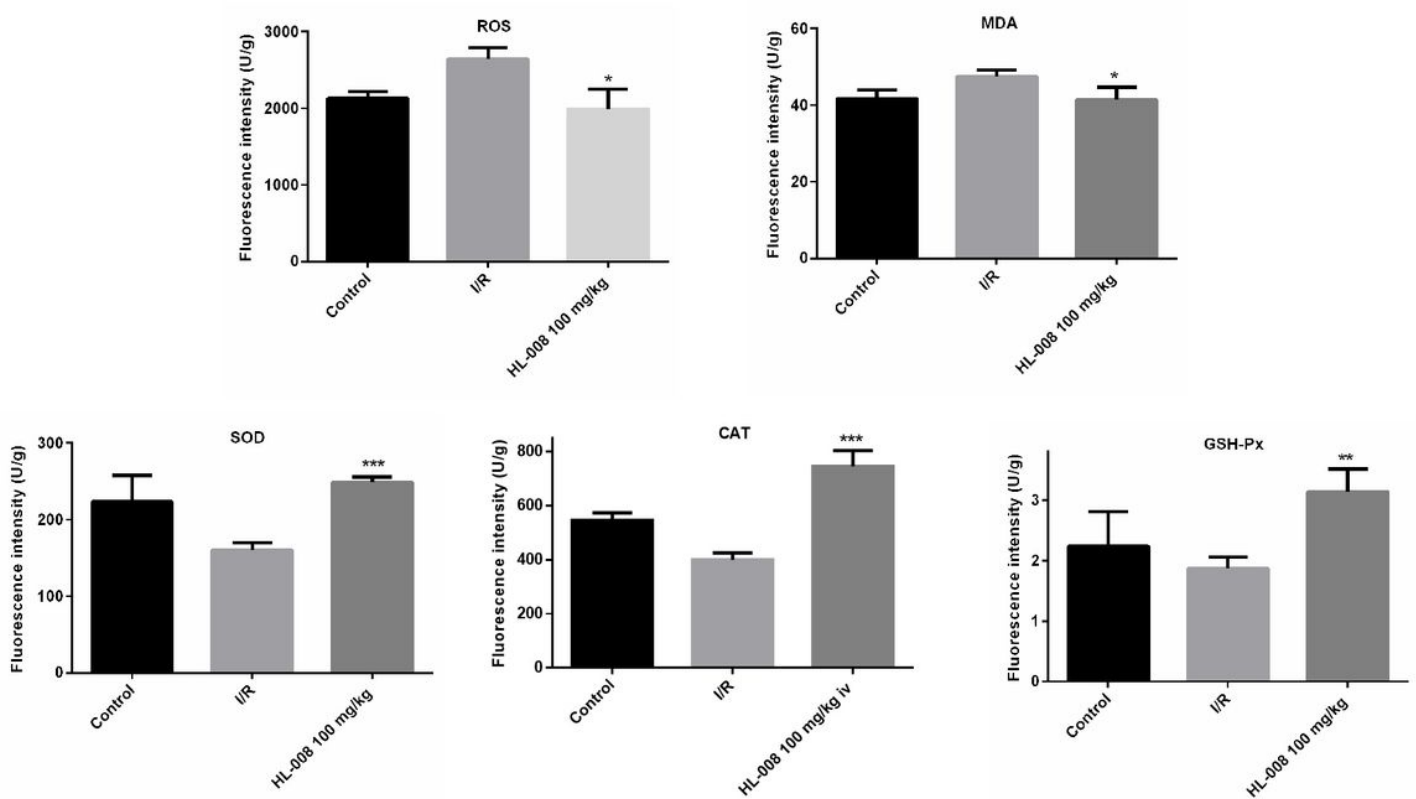


Figure 5

Evaluation of the effect of HL-008 on oxidation and antioxidant levels in the brain tissue of MCAO rats. The indices of oxidation level are: A, ROS level; B, MDA level. Antioxidant enzyme system indicators are: C, SOD level; D, CAT level; E, GSH-Px level. * $p < 0.05$, ** $p < 0.01$, *** $p < 0.001$.

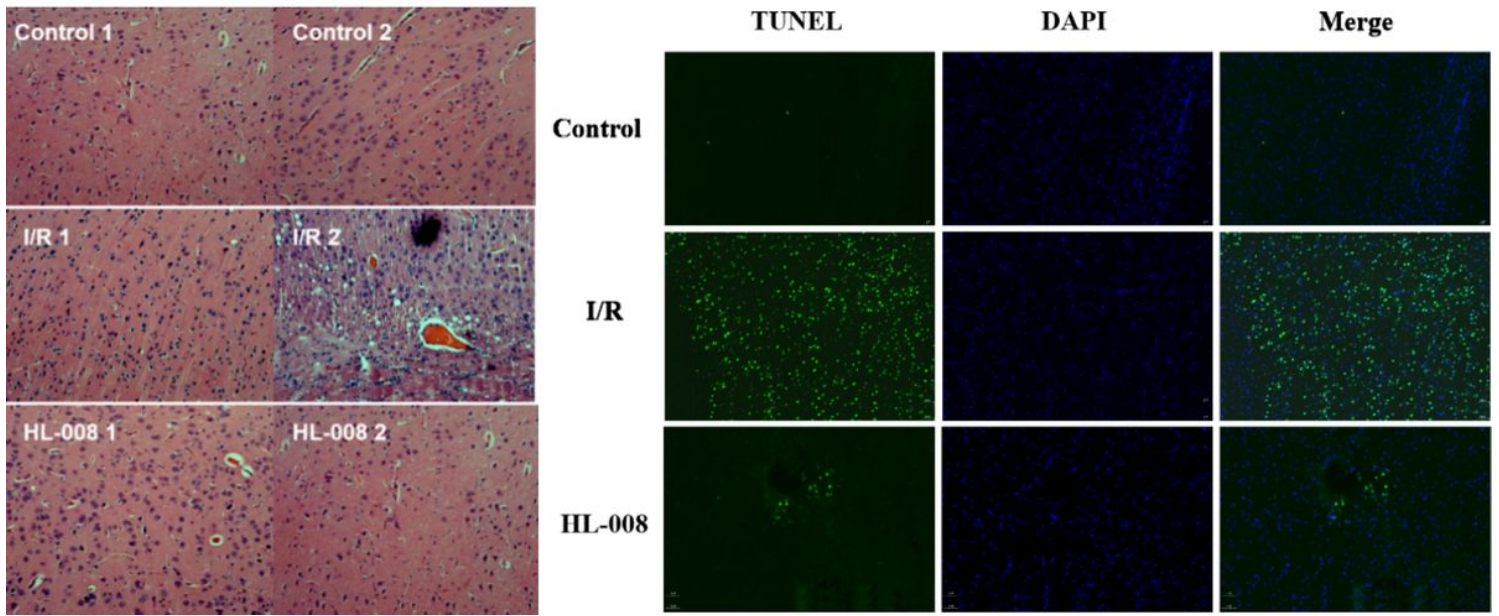


Figure 6

A. Effect of HL-008 on pathological changes in the brain tissue in MCAO rats evidenced by HE staining; B. The apoptotic cells were assessed using TUNEL staining. Green fluorescence represents TUNEL-positive cells.

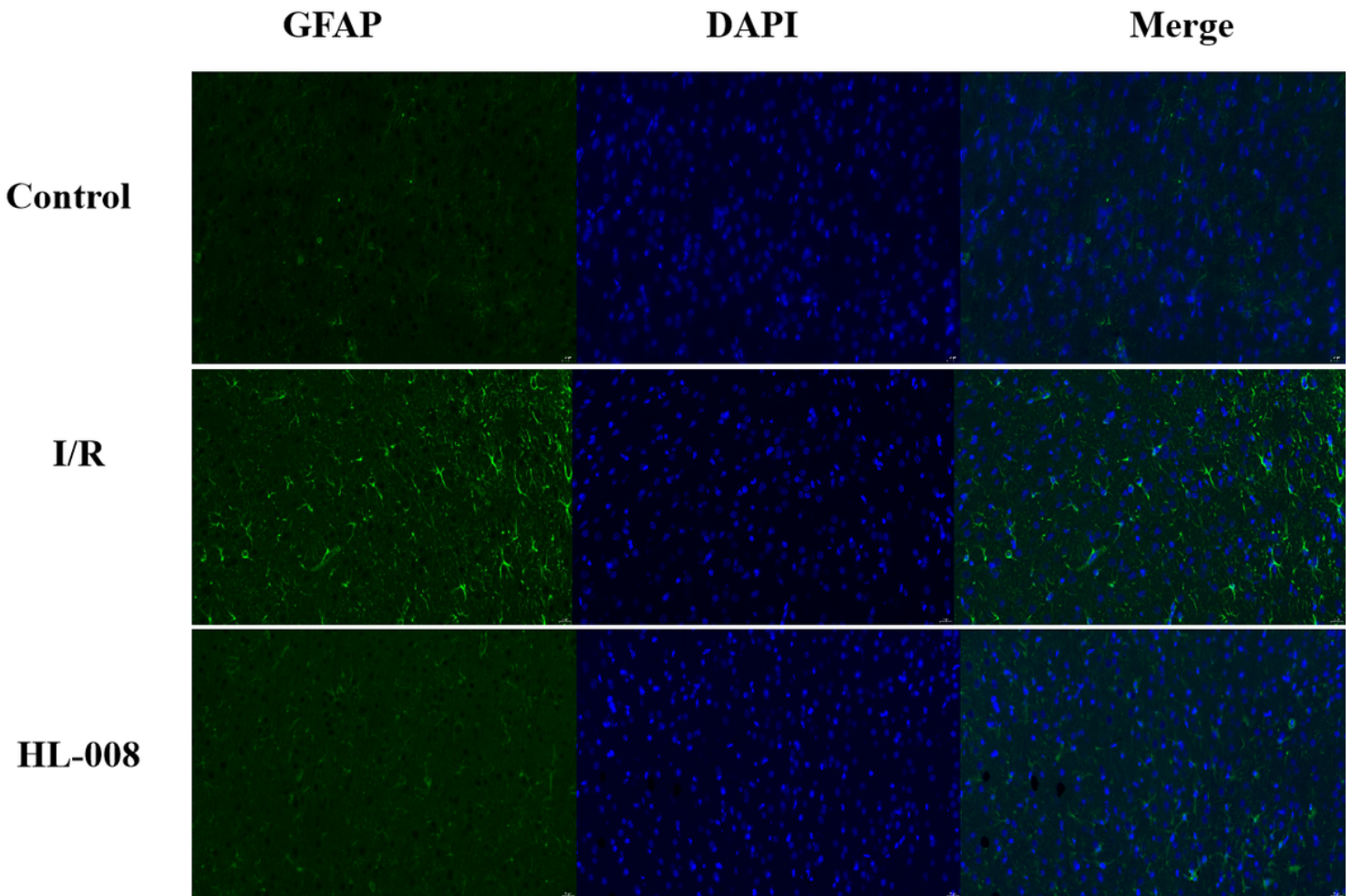


Figure 7

Effect of HL-008 on activation of astrocytes in the brain tissue of MCAO rats evaluated by fluorescence immunity.

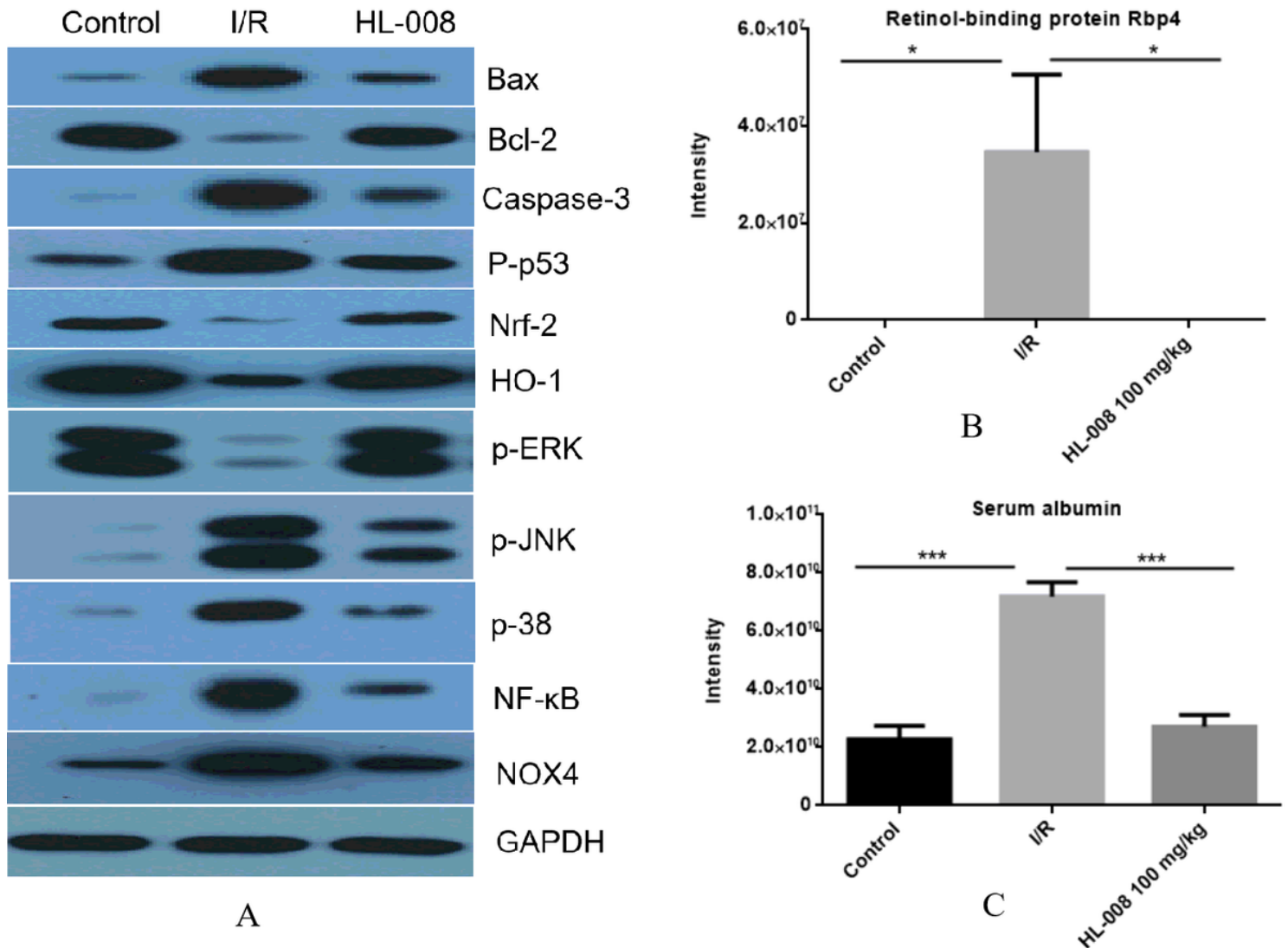


Figure 8

Effect of HL-008 on multiple signaling pathways in the brain tissue of MCAO rats. A. Western blot was used to detect the protein levels in the brain tissue of MCAO rats. The full-length gels were included in a Supplementary Information Figure S1. The protein expression was evaluated by proteomic analysis: B. Changes in the relational-binding protein in each group; C. Changes in serum albumin in each group.

Supplementary Files

This is a list of supplementary files associated with this preprint. Click to download.

- [Supplementarymaterials.docx](#)